Organic Electronics 40 (2017) 8–12

Contents lists available at ScienceDirect

Organic Electronics

journal homepage: www.elsevier.com/locate/orgel

Validation of opposed two-diode equivalent-circuit model for S-shaped characteristic in polymer photocell by low-light characterization

Kazuya Tada

Department of Electrical Materials and Engineering, University of Hyogo, 2167 Shosha, Himeji, Hyogo 671-2201, Japan

ARTICLE INFO

Article history:
Received 9 September 2016
Received in revised form
17 October 2016
Accepted 20 October 2016
Available online 26 October 2016

Keywords:
Photocell
Equivalent-circuit model
S-shaped curve
Bulk heterojunction composites
Indoor light harvesting
Polymer

ABSTRACT

The opposed two-diode equivalent-circuit model consisting of a traditional one-diode photocell model and a parasitic diode with a parallel resistance is known to somehow reproduce the S-shaped current-voltage curve of poor organic photocells. Here, the light-intensity dependencies of the parameters in the model are experimentally studied. On the assumption that the parasitic part is light-insensitive, the parameters of the main part, which are extracted by fitting the current-voltage curves under various illumination intensities with the model, are found to change as those of healthy photocells do. The reasonable separation of light-sensitive main and light-insensitive parasitic parts validates the model.

1. Introduction

Photocells based on printable organic materials are attracting much attention, because it is believed that they can be large-area low-cost renewable electric power source in the near future [1–4]. The S-shaped current-voltage characteristics are occasionally observed in the studies of such photocells using organic bulk heterojunction composite or bilayer. The S-shape is typically referred as a sign of poorly performing photocell, since it effectively reduces the fill-factor (FF) and thus the power conversion efficiency (PCE) of the photocell. Although the physical origin of the S-shaped characteristics is not fully understood, it has been pointed out that some deficiency between the layers, which potentially produces strong dipole or creates traps, and/or the unbalanced hole/electron mobility can cause the anomaly [5–10].

The opposed two-diode equivalent-circuit model shown in Fig. 1, which consists of a normal one-diode model for photocell and a parasitic opposed diode connected with a parallel resistance, has been known to somehow reproduce the S-shaped current-voltage characteristics [11,12]. Although the addition of the parasitic part is apparently intended to model the permanent deficiency that causes the S-shape, the physical origins of the parameters in the model have never been experimentally validated so far.

The transcendental nature of current-voltage equations for the model, which requires iterative calculation to solve, can be a serious barrier for the experimental researchers who are unfamiliar with code writing. However, the current-voltage relation of the model can be described by an exact expression by using the Lambert *W*-function $W_0(x)$ which is defined as the real solution of a simple transcendental equation $W(x)\cdot\exp[W\ (x)] = x$ for $x\in[-\exp(-1), +\infty]$ [13].

$$\begin{aligned} V =& I\cdot R_s - n_1\cdot V_t\cdot W_0\left\{\frac{I_{s1}\cdot R_{p1}}{n_1\cdot V_t}\cdot\exp\left(\frac{\left(I+I_{s1}+I_{ph}\right)\cdot R_{p1}}{n_1\cdot V_t}\right)\right\} \\ &+\left(I+I_{s1}+I_{ph}\right)\cdot R_{p1} \\ &+ n_2\cdot V_t\cdot W_0\left\{\frac{I_{s2}\cdot R_{p2}}{n_2\cdot V_t}\cdot\exp\left(\frac{-(I-I_{s2})\cdot R_{p2}}{n_2\cdot V_t}\right)\right\} \\ &+(I-I_{s2})\cdot R_{p2}, \end{aligned} \tag{1}$$

where I_{ph} is the ideal photocurrent, R_s and R_{p1} are the series and upper parallel (shunt) resistance respectively, and I_{s1} and n_1 are the

E-mail address: tada@eng.u-hyogo.ac.jp.

http://dx.doi.org/10.1016/j.orgel.2016.10.031
1566-1199/

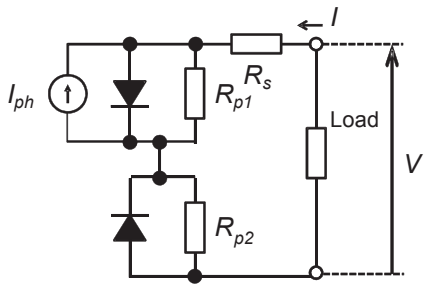

Fig. 1. Opposed two-diode equivalent-circuit model.

reverse saturation current and the ideality factor of the upper main diode respectively, in Fig. 1. The thermal voltage V_t at room temperature is 26 mV. The parameters with subscript 2 correspond to the lower parasitic part. Eq. (1) has been implemented in a Microsoft Excel spreadsheet which is provided as supporting information of the previous study [14], enabling one to estimate the circuit parameters by using Solver function of the program.

In this study, the low-light characteristics of a solution-processed polymer bulk heterojunction photocell, which shows S-shaped characteristics under AM1.5G 1 sun (100 mW/cm^2) illumination, are analyzed in order to investigate the light-intensity dependences of the parameters in the opposed two-diode equivalent-circuit model. The low-light characterization of photocell is becoming important issue in terms of the indoor light harvesting, where light power is typically lower than outdoor by 2–3 orders of magnitude [15–17]. Thus, the development of a suitable circuit model is not only helpful for understanding the device behavior, but also critically important for practical electronic circuit design.

2. Experimental

A bulk heterojunction photocell with ITO/PEDOT:PSS/PTB7-Th:C_{70} = 1:1/PFN/Al structure is used in this study, where ITO, PEDOT:PSS, PTB7-Th and PFN stand for indium-tin oxide, poly(3,4-dioxythiophene):poly(styrenesulfonate), poly[[4,8-bis[5-(2-ethylhexyl)thiophene-2-yl]benzo[1,2-b:4,5-b']dithiophene-2,6-diyl][3-fluoro-2-[(2-ethylhexyl)carbonyl]thieno[3,4-b]thiophenediyl]] [18,19] and poly[9,9-bis(3'-(*N*,*N*-dimethyl)-propyl-2,7-fluorene)-*alt*-2,7-(9,9-dioctylfluorene)], respectively. The schematic device structure as well as the molecular structures of the key materials is shown in Fig. 2. PTB7-Th and PFN are purchased from 1-materials and the active area of the devices is 3 mm × 3 mm square. The device preparation procedure is the same as that described in the previous study [20], except that the composite solution must be warmed on a hotplate heated at 100 °C for a few hours before spin-coating. This is simply due to lower solubility of the PTB7-Th sample used in the present study than that used in the previous study. Although the devices after the optimized thermal annealing yield the PCE close to 5% [20], the devices without thermal annealing show S-shaped current-voltage curve and are the target of the present study.

The current-voltage characteristics are measured with a Keithley 2400 source meter under the AM1.5G 1 sun illumination from an Asahi Spectra HAL-C100 solar simulator. The illumination light intensity is reduced by using a set of neutral density (ND) filters [21,22]. The reduction factors of the illumination light intensity are calculated by using the optical transmission spectra of the ND filters and the AM 1.5G 1 sun spectral data in the range of 350–750 nm [22].

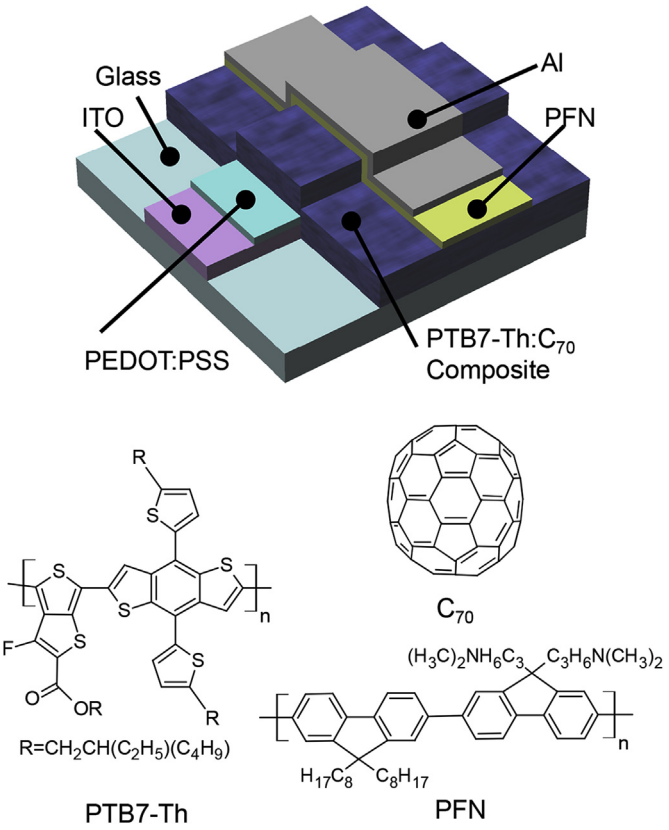

Fig. 2. Schematic structure of the photocell and molecular structures of key materials used in this study.

3. Results and discussion

The device shows typical S-shaped current-voltage characteristics under AM1.5G 1sun illumination as shown in Fig. 3. Since the device without thermal annealing in the previous study has shown normal current-voltage characteristics [20], and the S-shape disappears after the thermal annealing at 175 °C, this probably relates to some structural factor in the bulk and/or the surface of the composite film created by rapid cooling during the spin-coating. Table 1 summarizes the normalized circuit parameters obtained by fitting the data shown in Fig. 3 with the equivalent-circuit model

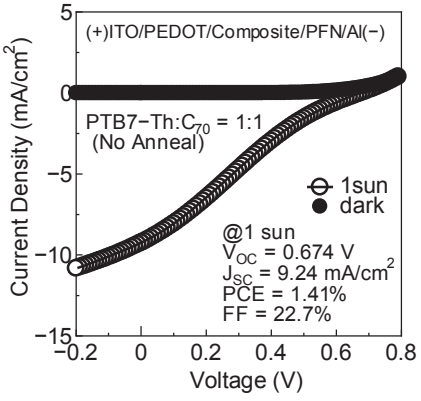

Fig. 3. Current density-voltage characteristics of the PTB7-Th:C_{70} photocell under AM1.5G 1 sun illumination and dark. The symbols and lines indicate experimental data and fitting curve, respectively.

Table 1
Normalized circuit parameters of the PTB7-Th:C_{70} photocells under AM1.5G 1 sun illumination extracted from the data in Fig. 3.

J_{ph} [mA/cm^2]	14.7
$R_{p1}\cdot A$ [Ω·cm^2]	99.9
$R_{p2}\cdot A$ [Ω·cm^2]	90.7
$R_s\cdot A$ [Ω·cm^2]	33.0
J_{s1} [nA/cm^2]	0.28
J_{s2} [nA/cm^2]	2.2×10^4
n_1	1.5 (fixed)
n_2	1.5 (fixed)

shown in Fig. 1. The ideality factors of the diodes are fixed to 1.5, which is typical for polymer photocells. Since relatively wide range of ideality factor can reproduce a single current-voltage curve of polymer photocells under illumination, especially for the S-shaped case [14,23], specific values of the ideality factors are not pursued.

As shown in Fig. 4(a), the dependence of the short-circuit photocurrent density (J_{SC}) of the device on illumination light intensity is sublinear and is expressed by a power function with a single exponent 0.90. It has been pointed out that the dependence cannot be described by a combination of linear and square-root dependences on the light intensity by A. Rose, who suggested that the exponential distribution of trap states near the band edge accounts for the sublinear dependence with a single exponent between 0.5 and unity [24,25].

On the other hand, the slope found in the semilogarithmic plot of the open-circuit voltage (V_{OC}) against the illumination light intensity shown in Fig. 4(b) is 34.6 mV. In the condition at which V_{OC} is measured, all photocarriers generated in the photocell are internally consumed. It has been reported that the slope equals to V_t in the trap-free case where the sole recombination path is bimolecular [21,26]. This is the ideal case where no other recombination processes such as those through traps and/or sub-edge states take place. The deviation of the value of the slope from the thermal energy can be referred as the degree of such recombination processes through traps and/or sub-edge states taking place in the photocell. Although it is probable that the slope relates to the level and the density of the traps and/or sub-edge states in the device, it seems that there is no generally-accepted equation which explicitly relates them. It should be worth to note that the parasitic part of the equivalent-circuit model does not contribute to V_{OC}, since current does not flow it under the open-circuit condition.

The FF significantly increases with decreasing the illumination light intensity as shown in Fig. 4(c). This is due to the disappearance of S-shape in current-voltage characteristic at reduced illumination. Thus, the PCE of the photocell increases with decreasing the illumination light intensity as shown in Fig. 4 (d). The PCE at 4×10^{-4} sun is found to be approximately 4.9%, which is more than three times of the PCE at 1 sun. Although the characteristic shown in Fig. 3 is apparently poor, the performance is significantly improved at low illumination light intensity.

Fig. 5 shows the normalized current density-voltage characteristics of the photocell. It is clearly indicated that the "S-shapeness" in the curve at 1 sun gradually weakens as the illumination intensity lowers. The circuit parameters in the upper main circuit are estimated as functions of the illumination light intensity by fitting the current-voltage curves with the opposed two-diode equivalent-circuit model. In this estimation, the parameters within the parasitic part are fixed to those indicated in Table 1. This means that the lower parasitic part in the circuit model is supposed to be light-insensitive. This is a natural assumption since it is unlikely that

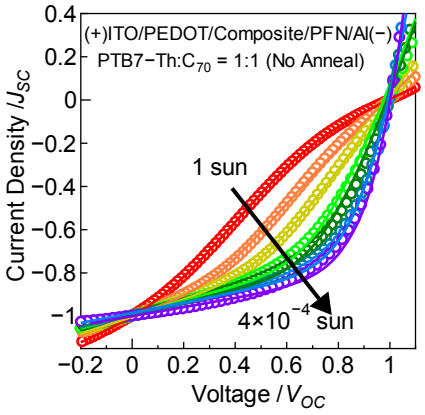

Fig. 5. Normalized current density–voltage characteristics at various illumination light intensities of the PTB7-Th:C_{70} photocell. The symbols and lines indicate experimental data and fitting curves, respectively.

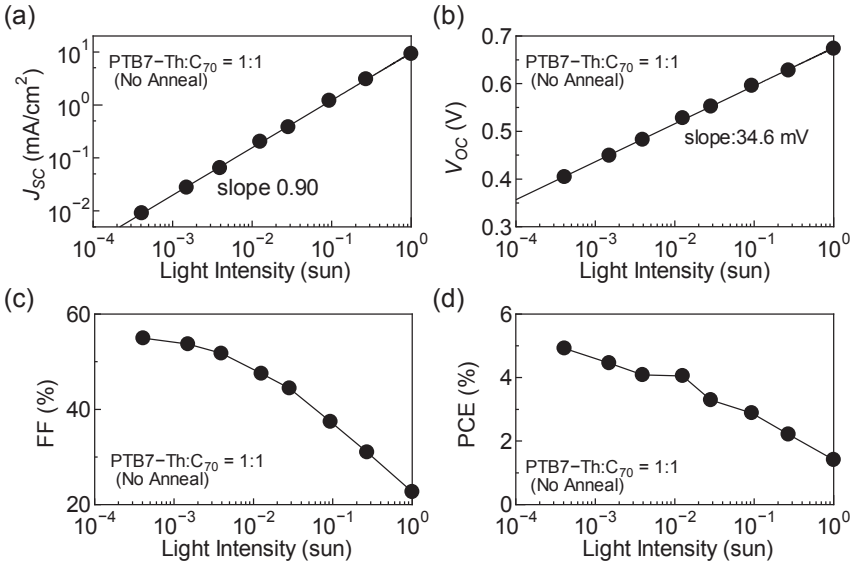

Fig. 4. Illumination light intensity dependences of (a) J_{SC}, (b) V_{OC}, (c) FF and (d) PCE of the PTB7-Th:C_{70} photocell.

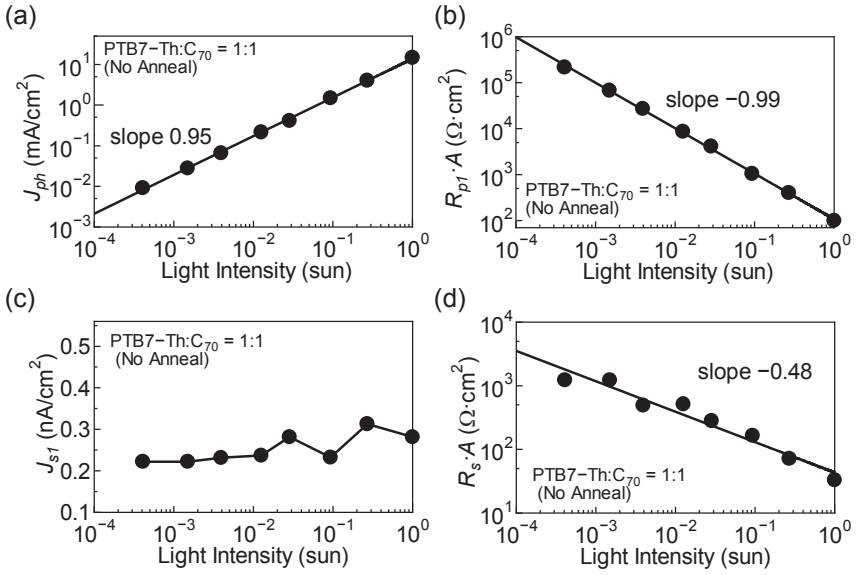

Fig. 6. Illumination light intensity dependences of (a) J_{ph}, (b) $R_p \cdot A$, (c) J_{s1} and (d) $R_s \cdot A$ of the PTB7-Th:C_{70} photocell without thermal annealing, where A stands for the active area of the photocell.

the illumination light intensities tested are high enough to modify the permanent deficiencies in the device. The successful fitting under the aforementioned condition strongly supports the validity of the opposed two-diode model, since the main and the parasitic parts are found to play their roles as naturally expected.

The circuit parameters estimated by the curve fitting are summarized in Fig. 6. The slope found in the double logarithmic plot of J_{ph} versus illumination light intensity shown in Fig. 6(a) is slightly increased from the slope observed in Fig. 4(a). The deviation may indicate that the photocarrier loss due to the interfacial deficiencies is separated. Namely, it is speculated that the apparent slope of 0.90 for the J_{SC} corresponds to the total loss of photocarriers in the device, while the slope of 0.95 for the J_{ph} corresponds to the loss in the composite bulk. The reciprocally proportional dependence of the parallel resistance in the main part of the model R_{p1} on the illumination light intensity shown in Fig. 6(b) can be explained by the photoconductive nature of the bulk heterojunction composite [27,28]. The J_{s1} remains almost constant in the present case as shown in Fig. 6(c). The aforementioned features basically coincide with those found in the healthy devices reported in the previously paper [22].

On the other hand, the R_s is found to have clear dependence on the illumination light intensity as shown in Fig. 6(d). In the case of healthy devices with small R_s, the fitting error becomes insensitive to the R_s at low illumination light intensity because the current through it also becomes small, making the precise identification of the R_s difficult. However, the fitting error in the present case is rather sensitive to the R_s even when the illumination light intensity is as low as 10^{-3} sun. Although the physical mechanism of the dependence is not clear at this stage, the sublinear dependence with a single exponent close to −0.5 suggests a certain relationship with the bimolecular recombination process of photocarriers. This indicates the importance of the R_s, although the factor is frequently ignored in the previous studies employing the opposed two-diode equivalent-circuit model, mainly for the sake of the reduction of computational effort [12,13,29].

4. Conclusion

In this study, the analysis of low-light characteristics of a polymer photocell, which shows S-shaped current-voltage curve at 1 sun, using the opposed two-diode equivalent-circuit model is carried out. It has been found that the light-intensity dependencies of the circuit parameters in the main part of the model are consistent with those in healthy devices, when the parasitic part is assumed to be light-insensitive as is naturally expected. The reasonable separation of light-sensitive and light-insensitive parts strongly supports the validity of the model. It is also demonstrated that the S-shape in the current-voltage characteristic at 1 sun of the polymer photocell disappears at reduced illumination light intensity. This means that apparently poor photocells showing the S-shaped curve at 1 sun are potentially useful for indoor applications.

Acknowledgements

This work was partially supported by JSPS KAKENHI Grant Number JP26289094.

References

[1] A.J. Heeger, Bulk heterojunction solar cells: understanding the mechanism of operation, Adv. Mater. 26 (2014) 10–28.
[2] G. Li, R. Zhu, Y. Yang, Polymer solar cells, Nat. Phot. 6 (2012) 153–161.
[3] F.C. Krebs, Fabrication and processing of polymer solar cells: a review of printing and coating techniques, Sol. Ener. Mater. Sol. Cells 93 (2009) 394–412.
[4] R. Po, A. Bernardi, A. Calabrese, C. Carbonera, G. Corso, A. Pellegrino, From lab to fab: how must the polymer solar cell materials design change? – an industrial perspective, Energy Environ. Sci. 3 (2010) 512–525.
[5] A. Kumar, S. Sista, Y. Yang, Dipole induced anomalous S-shape I–V curves in polymer solar cells, J. Appl. Phys. 105 (2009), 094512-1–094512-3.
[6] D. Gupta, M. Bag, K.S. Narayan, Correlating reduced fill factor in polymer solar cells to contact effects, Appl. Phys. Lett. 92 (2008), 093301-1–093301-3.
[7] A. Wagenpfahl, D. Rauh, M. Binder, C. Deibel, V. Dyakonov, S-shaped current-voltage characteristics of organic solar devices, Phys. Rev. B 82 (2010), 115306-1–115306-8.
[8] B.Y. Finck, B.J. Schwartz, Understanding the origin of the S-curve in conjugated polymer/fullerene photovoltaics from drift-diffusion simulations, Appl. Phys. Lett. 103 (2013), 053306-1–053306-3.
[9] W. Tress, A. Petrich, M. Hummert, M. Hein, K. Leo, M. Riede, Imbalanced mobilities causing S-shaped IV curves in planar heterojunction organic solar cells, Appl. Phys. Lett. 98 (2011), 063301-1–063301-3.
[10] A. Gusain, S. Singh, A.K. Chauhan, V. Saxena, P. Jha, P. Veerender, A. Singh, P.V. Varde, S. Basu, D.K. Aswal, S.K. Gupta, Electron density profile at the interfaces of bulk heterojunction solar cells and its implication on the S-kink characteristics, Chem. Phys. Lett. 646 (2016) 6–11.

[11] F.A. de Castro, J. Heier, F. Nüesch, R. Hany, Origin of the kink in current-density versus voltage curves and efficiency enhancement of polymer-C heterojunction solar cells, IEEE J. Sel. Top. Quant. Electron 16 (2010) 1690–1699.
[12] G. del Pozo, B. Romero, B. Arredondo, Evolution with annealing of solar cell parameters modeling the S-shape of the current-voltage characteristic, Sol. Energy Mater. Sol. Cells 104 (2012) 81–86.
[13] B. Romero, G. del Pozo, B. Arrendondo, Exact analytical solution of a two diode circuit model for organic solar cells showing S-shape using Lambert W-functions, Sol. Energy 86 (2012) 3026–3029.
[14] K. Tada, Parameter extraction from S-shaped current-voltage characteristics in organic photocell with opposed two-diode model: effects of ideality factors and series resistance, Phys. Stat. Solidi (a) 212 (2015) 1731–1734.
[15] J.F. Randall, J. Jacot, Is AM1.5 applicable in practice? Modelling eight photovoltaic materials with respect to light intensity and two spectra, Renew. Energy 28 (2003) 1851–1864.
[16] S. Mori, T. Gotanda, Y. Nakano, M. Saito, K. Todori, M. Hosoya, Investigation of the organic solar cell characteristics for indoor LED light applications, Jpn. J. Appl. Phys. 54 (2015) 071602.
[17] H.K.H. Lee, Z. Li, J.R. Durrant, W.C. Tsoi, Is organic photovoltaics promising for indoor applications? Appl. Phys. Lett. 108 (2016) 253301.
[18] S.-H. Liao, H.-J. Jhuo, Y.-S. Cheng, S.-A. Chen, Fullerene derivative-doped zinc oxide nanofilm as the cathode of inverted polymer solar cells with low-bandgap polymer (PTB7-Th) for high performance, Adv. Mater. 25 (2013) 4766–4771.
[19] H. Zhou, Y. Zhang, C.-K. Mai, S.D. Collins, G.C. Bazan, T.-Q. Nguyen, A.J. Heeger, Polymer homo-tandem solar cells with best efficiency of 11.3%, Adv. Mater. 27 (2015) 1767–1773.
[20] K. Tada, Solution-processed photocells based on low energy-gap polymer and unmodified C_{70} composites from halogen-free solvent exceeding 5% power conversion efficiency, Sol. Energy Mater. Sol. Cells 143 (2015) 52–57.
[21] S.R. Cowan, A. Roy, A.J. Heeger, Recombination in polymer-fullerene bulk heterojunction solar cells, Phys. Rev. B 82 (2010), 245207-1–245207-10.
[22] K. Tada, Characterization of polymer bulk heterojunction photocell with unmodified C_{70} prepared with halogen-free solvent for indoor light harvesting, Org. Electron 30 (2016) 289–295.
[23] K. Tada, Effect of conjugated polyelectrolyte interlayer at cathode in bulk heterojunction photocells based on neat C_{70} and low-energy-gap polymer prepared with halogen-free solvent, Appl. Phys. Express 7 (2014), 051601-1–051601-4.
[24] A. Rose, An outline of some photoconductive processes, RCA Rev. 12 (1951) 362–414.
[25] A. Rose, Concepts in Photoconductivity and Allied Problems, Wiley, New York, 1963.
[26] L.J.A. Koster, V.D. Mihailetchi, R. Ramaker, P.W.M. Blom, Light intensity dependence of open-circuit voltage of polymer:fullerene solar cells, Appl. Phys. Lett. 86 (2005), 123509-1–123509-3.
[27] P. Schilinsky, C. Waldauf, J. Hauch, C.J. Brabec, Simulation of light intensity dependent current characteristics of polymer solar cells, J. Appl. Phys. 95 (2004) 2816–2819.
[28] C. Waldauf, P. Schilinsky, J. Hauch, C.J. Brabec, Material and device concepts for organic photovoltaics: towards competitive efficiencies, Thin Solid Films 451–452 (2004) 503–507.
[29] B. Romero, G. Del Pozo, E. Destouesse, S. Chambon, B. Arredondo, Circuital modelling of S-shape removal in the current-voltage characteristic of TiO_x inverted organic solar cells through white-light soaking, Org. Electron 15 (2014) 3546–3551.